

1 Article

2 Compatibility of aerial and terrestrial LiDAR for 3 quantifying forest structural diversity

4 **Elizabeth A. LaRue¹*, Franklin W. Wagner¹#, Songlin Fei^{1*}, Jeff W. Atkins², Robert T. Fahey³,
5 Chris M. Gough², Brady S. Hardiman^{1,4}**

6 ¹ Dept. of Forestry & Natural Resources, Purdue University, 715 W. State Street, West Lafayette, IN 47907;
7 sfei@purdue.edu

8 ² Dept. of Biology, Virginia Commonwealth University, 1000 W. Cary Street, Richmond, VA 23284;
9 cmgough@vcu.edu

10 ³ Dept. of Natural Resources and the Environment and Center for Environmental Sciences and Engineering,
11 University of Connecticut, 1376 Storrs Road, Storrs, CT 06269; robert.fahey@uconn.edu

12 ⁴ Div. of Environmental and Ecological Engineering, Purdue University, 715 W. State Street, West Lafayette,
13 IN 47907; bhardima@purdue.edu

14 * These authors contributed equally

15 * Correspondence: sfei@purdue.edu; Tel.: +1-765-496-2199

16 Received: date; Accepted: date; Published: date

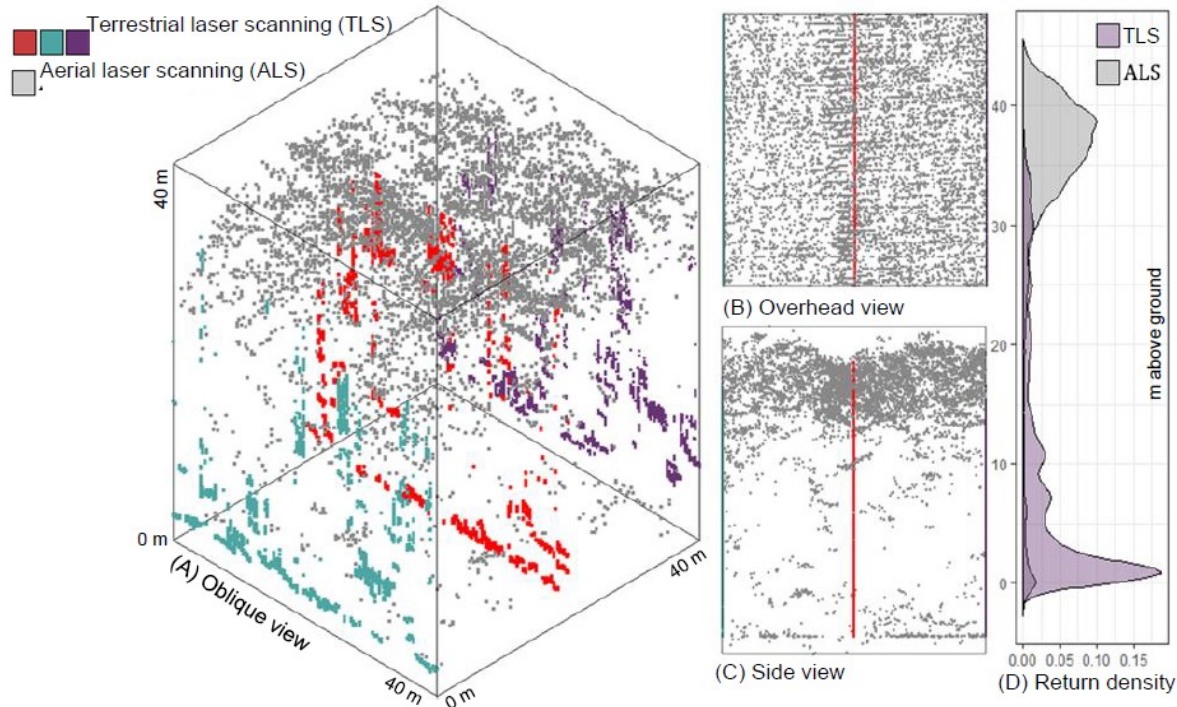
17 **Abstract:** Structural diversity is a key feature of forest ecosystems that influences ecosystem
18 functions from local to macroscales. The ability to measure structural diversity in forests with
19 varying ecological composition and management history can improve the understanding of
20 linkages between forest structure and ecosystem functioning. Terrestrial LiDAR has often been used
21 to provide a detailed characterization of structural diversity at local scales, but it is largely unknown
22 whether these same structural features are detectable using aerial LiDAR data that are available
23 across larger spatial scales. We used univariate and multivariate analyses to quantify cross-
24 compatibility of structural diversity metrics from terrestrial versus aerial LiDAR in seven National
25 Ecological Observatory Network sites across the eastern USA. We found strong univariate
26 agreement between terrestrial and aerial LiDAR metrics of canopy height, openness, internal
27 heterogeneity, and leaf area, but found marginal agreement between metrics that describe
28 heterogeneity of the outer most layer of the canopy. Terrestrial and aerial LiDAR both demonstrated
29 the ability to distinguish forest sites from structural diversity metrics in multivariate space, but
30 terrestrial LiDAR was able to resolve finer-scale detail within sites. Our findings indicate that aerial
31 LiDAR can be of use in quantifying broad-scale variation in structural diversity across macroscales.

32 **Keywords:** ALS; Forest Ecology; Forest Structure; NEON; Macrosystems Biology; TLS
33

34 1. Introduction

35 Forest structural diversity is the physical arrangement and variability of the living and non-
36 living biotic elements within forest stands, that support many essential ecosystem functions [1]. As
37 a critical driver of forest function, estimates of structural diversity are a useful proxy for predicting
38 forest ecosystem functions. For example, structural diversity can be used to predict light
39 interception [2], microclimate [3], hydrology [4], and resilience to disturbance [5]. Forest structural
40 diversity arises from the complex interactions of a range of abiotic and biotic factors that influence
41 the growth and the quantity of vegetation [6–8]. A wide variety of structural diversity metrics can
42 be estimated using methods that range from traditional forest inventory approaches (e.g. basal area
43 [9]) to next-generation remote sensing techniques (e.g. canopy traits or multivariate structural types
44 [7]). The complex and dynamic nature of forest structure has proven challenging to measure

45 accurately across scales and forest structure types [10,11], but such measurements could
 46 substantially improve predictions of forest ecosystem functions [12].



47
 48 **Fig. 1.** Comparison of aerial laser scanning (ALS) and terrestrial laser scanning (TLS) point clouds for
 49 the Great Smoky Mountains site of the National Ecological Observatory Network at plot 053 (40 x 40
 50 m) from oblique (A), overhead (B), and side angles (C). Vertical profiles of return heights from raw
 51 LiDAR returns (D) demonstrate the occlusion experienced by both LiDAR methods as a result of their
 52 respective view angles (return density refers to the proportion of total points or relative densities of
 53 returns from each platform).

54
 55 LiDAR remote sensing may be particularly useful in quantifying structural diversity by
 56 providing detailed three-dimensional data on the vegetative features and canopy elements within
 57 forest stands, but each LiDAR platform has trade-offs in resolution [13]. LiDAR is a useful tool for
 58 the multi-dimensional characterization of forest structure that has versatile terrestrial and aerial
 59 deployment platforms spanning a multiple of spatial extents and resolutions [14–18]. Terrestrial laser
 60 scanning (TLS) and aerial laser scanning (ALS) have both been shown to be effective at quantifying
 61 components of forest structural diversity [14–20], however, each LiDAR platform has trade-offs for
 62 data resolution and spatial coverage. Stationary TLS instruments and ALS scan the forest from
 63 opposite angles and occlusion by the canopy constrains the capacity of each to obtain data from
 64 portions of the canopy distal to the instrument [21] (Fig. 1). TLS measures the forest from within,
 65 providing high resolution data on complex, fine-scale internal features of canopy structural diversity
 66 [22]. However, TLS data are less reliable for the upper canopy due to occlusion by intervening foliage
 67 [23]. Conversely, ALS measures the forest from above, providing the highest level of detail on the
 68 outer canopy surface with declining capacity to resolve canopy features with increasing canopy
 69 depth [23]. ALS can delineate vertical stratification and understory layers of vegetation [24], but the
 70 accuracy of measuring the sub-canopy with ALS can depend upon the orientation of the overstory

71 [25] and the metrics being used [26,27]. Furthermore, it has been shown that ALS instrumentation
72 specifications, such as point density, can influence the ability to access sub-canopy elements [28,29].

73 Despite past work examining whether it is possible to obtain similar estimates of structural
74 diversity with high density TLS data and low density ALS data [23,30–32], little is known about how
75 these compare across ecologically heterogeneous macroscales. TLS and ALS may not always be able
76 to resolve the same aspects or metrics of structural diversity well due to their opposing viewing
77 angles [23,33]. Previous studies within a single site or forest type dominated by one tree species
78 demonstrated that TLS and ALS estimates of forest structural diversity were correlated [23,34–36].
79 However, forests vary in structure and species composition substantially from local to regional scales
80 [37]. The ability to scale high resolution TLS metrics of structural diversity with spatially extensive
81 ALS data could help improve the understanding of links between structural diversity and ecosystem
82 function across scales. It is therefore necessary to compare their ability to estimate forest structural
83 diversity across different forest types that may vary in their structural types within ecologically
84 heterogeneous macroscales.

85 We compared the quantification of structural diversity using metrics from TLS and ALS
86 across seven forested sites in the eastern USA from the National Ecological Observatory Network
87 (NEON) (Table 1, Fig. 2). We focused on the types of structural diversity metrics (i.e. canopy
88 structural traits) that can be measured by LiDAR methods. First, we examined the univariate
89 correlations of computationally comparable ALS and TLS structural diversity metrics. Second, we
90 tested for intercorrelations between ALS and TLS suites of structural diversity metrics. Third, we
91 compared the multivariate suites of ALS and TLS structural diversity metrics to compare their
92 relative abilities to categorize plots from different forest types. Our study results have implications
93 for providing a reliable remote sensing toolkit for linking structural diversity and ecosystem
94 functions in forest macrosystems.

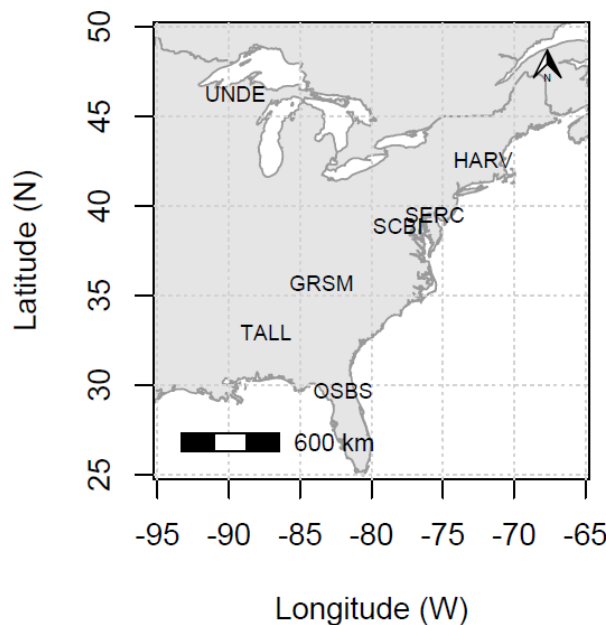
95

96

97

98

99



100
101 **Fig. 2.** Seven forested sites (see Table 1 for site descriptions) from the National Ecological
102 Observatory Network across the eastern USA measured by aerial laser scanning (ALS) and
103 terrestrial laser scanning (TLS).

104
105 **Table 1.** Seven forested National Ecological Observatory Network sites measured using both
106 terrestrial laser scanning (TLS) and aerial laser scanning (ALS).

Site (ID)	Ecoclimatic domain	Dominant forest type	NPlots
Harvard Forest (HARV)	Northeast	Mixed temperate	19
Smithsonian Conservation Biology Institute (SCBI)	Mid-Atlantic	Mixed temperate	6
Smithsonian Environmental Research Center (SERC)	Mid-Atlantic	Temperate deciduous	13
Ordway-Swisher Biological Station (OSBS)	Southeast	Pine Savannah	20
University of Notre Dame Environmental Research Center East (UNDE)	Great Lakes	Mixed temperate	8
Great Smoky Mountain National Park (GRSM)	Appalachians & Cumberland Plateau	Temperate rainforest	10
Talladega National Forest (TALL)	Ozarks Complex	Pine savannah	12

109 **2. Materials and Methods**110 **2.1 LiDAR Data Collection and structural diversity metrics**

111 To evaluate the potential for combining TLS and ALS structural diversity metrics into a more
 112 comprehensive assessment of forest structural diversity at large spatial scales, we analyzed data
 113 acquired using both platforms within 40 m x 40 m distributed sampling plots (n = 88) at seven NEON
 114 sites in the eastern USA (Table 1, Fig. 2). These sites are located in 6 ecoclimatic domains that span a
 115 wide gradient of structural diversity and forest community composition. Structural diversity metrics
 116 derived from both ALS and TLS are grouped into four different categories that all describe traits of
 117 the canopy [10]. These categories include: (1) *canopy height*, (2) *canopy cover and openness*, and (3) *canopy*
 118 *heterogeneity* (internal and external; [1]), and (4) *vegetation area*.

119

120 **Table 2.** Categories of forest structural diversity and metrics from terrestrial laser scanning (TLS) and
 121 aerial laser scanning (ALS) platforms. Details on the derivation and R functions used to calculate
 122 structural metrics can be found in Atkins et al. [10] for TLS and Table S1 for ALS. The abbreviations
 123 of metric names are listed in parentheses.

Category	ALS metric	TLS metric
Height	Mean canopy height (H), Mean outer canopy height (MOCH), Maximum canopy height (Hmax)	Mean leaf height (Mean H), Mean outer canopy height (MOCH), Maximum canopy height (Max.can.ht), Mean of squared leaf height model (Mode.2), Mode.el (Model.el), Mean height of maximum VAI (Max.el), Root mean square height (meanHRMS), Mean height variability (meanHvar), SD of mean height (Height.2)
Cover and openness	Deep gaps (DG), Deep gap fraction (DGF), Cover fraction (CF), Gap fraction profile (GFP)	Deep gaps (DG), Deep gap fraction (DGF), Sky fraction (SF), Cover fraction (CF)
Heterogeneity	External	Top rugosity (TR), Rumple (Rumple)
	Internal	SD of vertical SD of height (StdStd), Entropy (Entropy), Height SD (HSD: rLiDAR), Height SD (StdH: lidR), Vertical complexity index (VCI)
Vegetation area	Vegetation area index (VAI)	Mean VAI (Mean.VAI), Mean peak VAI (Mean.peak.VAI)

124

125 We measured canopy structural diversity with 21 different metrics (Table 2) from TLS data.
 126 TLS data were collected using a portable canopy LiDAR (a type of TLS) (Riegl LD90-3100VHS-FLP;
 127 Table 3) from each site in summer 2016. The system consists of an upward facing 900 nm laser

128 rangefinder mounted on a wearable frame that is moved along a 40 m pre-defined transect through
 129 the plot. The data collected corresponds to a vertical two-dimensional cross section through the
 130 canopy with approximately 500–2,000 data points collected per linear meter (Fig. 1). The full
 131 description of the design, operation, and validation of the TLS system is found in Parker et al. [22].
 132 For this study, three parallel transects of 40 m each in length were measured per NEON plot (Fig. 1A;
 133 see [2] for data collection methods). In order to reduce seasonal differences in forest structural
 134 diversity, plots were sampled at each site at or very near peak greenness; the exact dates of sampling
 135 for each site can be found in Atkins et al. [38]. This TLS data was then used to characterize canopy
 136 structural diversity from a suite of 21 metrics (Table 2) in the *forestr 1.0.1* package [10] in R v.3.5.2 [39],
 137 which creates 1 m² bins of returns along the 40 m 2D LiDAR point cloud to quantify the 21 structural
 138 diversity metrics.

139 **Table 3.** LiDAR system specifications for aerial laser scanning (ALS) and terrestrial laser scanning
 140 (TLS) platforms.

System Specifications	Optech ALTM Gemini (ALS)	Riegl LD90-3100VHS-FLP (TLS)
Returns per Pulse	Four	Five
Wavelength	1064 nm	900 nm
Measurement Range	150–4000 m	60 m ($\rho \geq 0.1$)–200 m ($\rho \geq 0.8$)
Range Accuracy (typical)	± 5 –30 cm	± 2.5 cm
Beam Divergence Angle	0.25 mrad \times 0.8 mrad	3 mrad \times 5 mrad
Measurement Rate (per second)	0–70 (programmable)	2,000
Average Point Density	1 - 4 points per m ²	500–2,000 points per linear meter
Laser Product Classification	Class IV (US FDA 21 CFR)	IEC 60825–1:2007 (Eye-safe)

141
 142 We derived a suite of 15 structural diversity metrics (Table 2) from level-1 discrete return
 143 ALS data (Product No. DP1.30003.001) that is collected by the NEON Aerial Observation Platform.
 144 This ALS consists of a 1,064 nm whiskbroom scanning laser (Optech ALTM Gemini; Table 3) flown
 145 over the study sites at 1,000 m above ground level, producing a three-dimensional point cloud with
 146 a final point density of 1–4 points m² (Table 3). Detailed methods on the NEON ALS data collection
 147 methods and all data can be found on the NEON Data Portal [40]. ALS data were collected for each
 148 site in 2016 (TALL, OSBS, GRSM, HARV, UNDE) or 2017 (SCBI, SERC). All NEON Aerial
 149 Observation Platform data is collected during peak growing season (maximum canopy greenness).
 150 The exact dates for data collection of ALS data used here are available through the NEON data portal
 151 [40]. Extreme outlier points were visually screened in the 1 km².laz files provided by NEON and if
 152 outliers were found they were manually filtered out using the *readLAS* function in the *lidR* package
 153 [41]. Return heights were corrected for topographic variation using a digital terrain model (DTM).
 154 The DTM was created from the *grid_terrain* function and was then used to correct return heights for

155 topographic variation in the *lasnormalize* function of the *lidR* package [41]. A 100 m buffer zone was
156 included around each plot center to minimize potential edge effects when correcting for topographic
157 variation. A point cloud encompassing the 1,600 m² plot area was then clipped from the buffer point
158 cloud. We used the *lidR* [41] and *rLiDAR* R packages [42] to measure 15 structural diversity metrics
159 (Table 2). The definitions and R functions used to calculate each of the 15 structural diversity metrics
160 are found in Table S1. There were fewer ALS than TLS metrics because the point density of ALS is
161 much lower than TLS. Therefore, low density ALS cannot be used to describe some of the TLS metrics
162 that require fine-scale data on the absence of laser pulses intersecting vegetation in the subcanopy
163 (e.g. the porousness of gaps between vegetative materials such as leaves [10]). Finally, we compared
164 the data collection methods of ALS and TLS, by measuring the distance at which structural diversity
165 metrics stabilized from slices of varying widths taken from ALS data (see the Supplemental
166 Information Section 1). The analysis supported our approach of averaging multiple 2D canopy slices
167 of TLS data to estimate plot structural diversity, so that we could then compare these values to whole
168 plot ALS metrics of structural diversity.

169 2.2 Data Analysis

170 To investigate the univariate strength and direction of correlations between ALS and TLS
171 structural diversity metrics, we calculated a non-parametric Spearman's correlation coefficient (r)
172 between equivalently estimated structural diversity metrics and each pairwise combination of
173 metrics between LiDAR platforms. To facilitate interpretation, we considered an $|r| \geq 0.7$ as a strong
174 correlation, $|r| \geq 0.5$ as a moderate correlation, and a $|r| \leq 0.5$ as a weak correlation.

175 We performed multivariate analyses to assess differentiation in the clustering of plots from
176 different sites based on all the structural diversity metrics provided by the two LiDAR methods. First,
177 we performed non-metric multidimensional scaling (NMS) ordination on plot-level data sets of the
178 TLS and ALS suites of structural diversity metrics. Ordinations were conducted in PC-ORD v.5.31
179 [43] with Sorenson's distance measure and the "slow-and-thorough" auto-pilot setting, using 250
180 runs of real data and 250 Monte Carlo randomizations to assess the robustness of the solution [44].
181 Ordinations were conducted on matrices with all metrics first relativized to the maximum value that
182 the metric obtained to scale all metrics equivalently. We tested for differences among groupings in
183 each data set (TLS, ALS) in multivariate suites of canopy structural metrics using Multiple Response
184 Permutation Procedure (MRPP) with Sorenson's distance measure in PC-ORD [44]. We performed
185 hierarchical agglomerative clustering on matrices of structural diversity metrics to determine
186 clustering of plots into canopy structural types [7]. Clustering was performed with PC-ORD using
187 Ward's Method and Euclidean distance measures [44]. The optimal cluster grouping level was
188 determined by conducting Indicator Species Analysis and deriving mean p-values for indicator
189 values across all metrics for each level of grouping [44]. The grouping level with the lowest mean p-
190 value was selected as the optimal grouping level or cluster for the data [44]. Finally, we compared
191 the classification of plots between the ALS and TLS-derived classifications by creating a confusion
192 matrix with TLS classifications utilized as the "ground-truth" data for assessing the classification
193 produced by the ALS system.

194 3. Results

195 3.1 Univariate Comparison of ALS and TLS Metrics

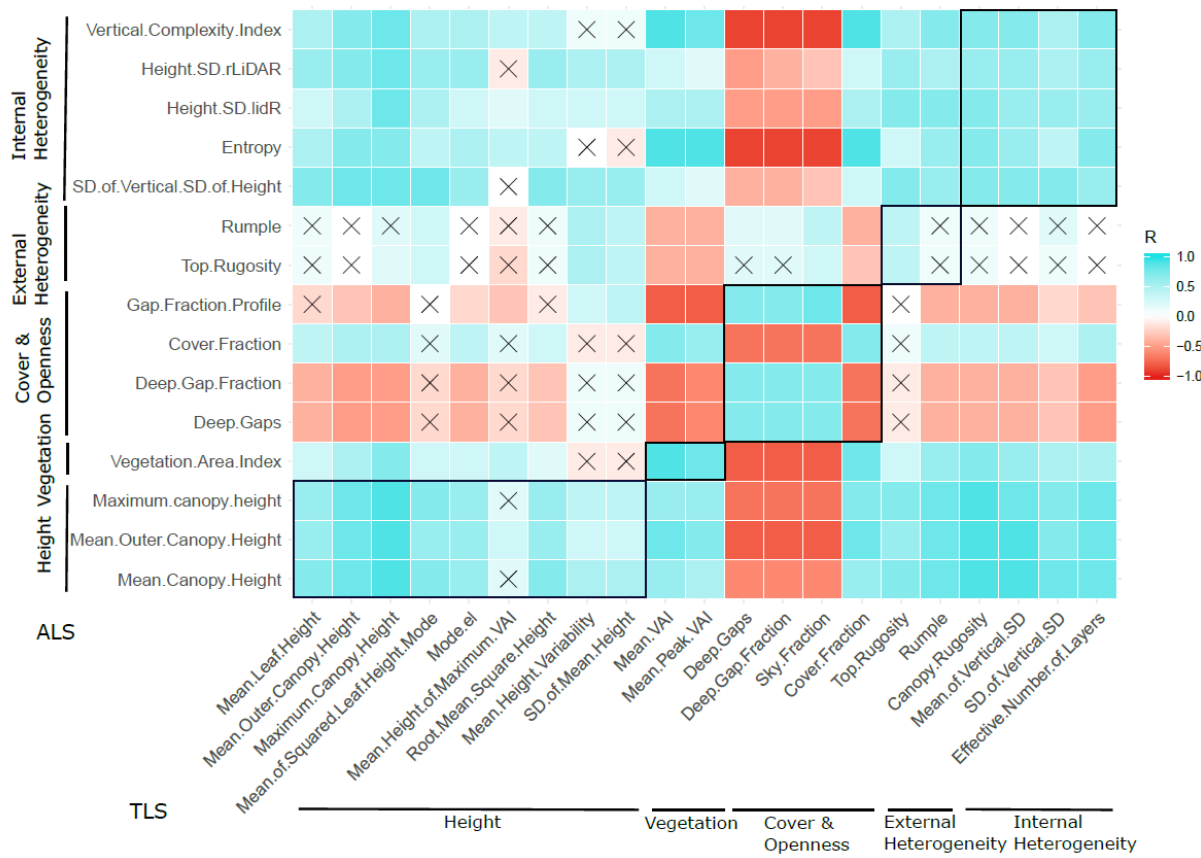
Many metrics from ALS and TLS were correlated ($r = 0.44\text{--}0.92$) within and across structural diversity categories (Fig. 3). First, there were significant moderate to strong correlations of $r > 0.6$ among eight metrics that have equivalent measurements of the same structural aspect of canopies (Table 4). The only exception was in the category of external heterogeneity, where there was a weak significant correlation between ALS and TLS metrics of top rugosity ($r = 0.44$), but not rumple ($r = 0.09$) (Table 4, Fig. 3). Second, ALS and TLS metrics within the same category of structural diversity, but not necessarily the equivalent measurement of the same metric, varied in how strongly they were correlated (Fig. 3). Height and vegetation area metrics were both moderately to strongly positively correlated (Fig. 3). Cover and openness metrics were strongly correlated between TLS and ALS (Fig. 3). When comparing ALS and TLS, heterogeneity metrics were much more variable in their correlation strength, which varied from neutral to strongly positively correlated (Fig. 3). Third, there was significant and frequent intercorrelation among metrics of structural diversity from different categories (Fig. 3). Overall, this analysis suggests that ALS-derived metrics of structural diversity can provide statistically similar estimates of structural diversity compared to TLS, though the accuracy of these estimates vary depending on the specific structural metric.

211

Table 4. Spearman correlations between equivalently estimated structural diversity metrics with terrestrial laser scanning (TLS) and aerial laser scanning (ALS). * indicates that values were significant at $\alpha < 0.05$.

Category	ALS	TLS	r
Height	MOCH	MOCH	0.80*
	H	H	0.72*
	Hmax	Max.can.ht	0.92*
Cover and openness	DGF	DGF	0.66*
	CF	CF	0.74*
External heterogeneity	Rumble	Rumble	0.09
	TR	TR	0.44*
Internal heterogeneity	StdH	MeanStd	0.61*
	StdStd	Rugosity	0.74*
Vegetation area	VAI	VAI	0.87*

215



216

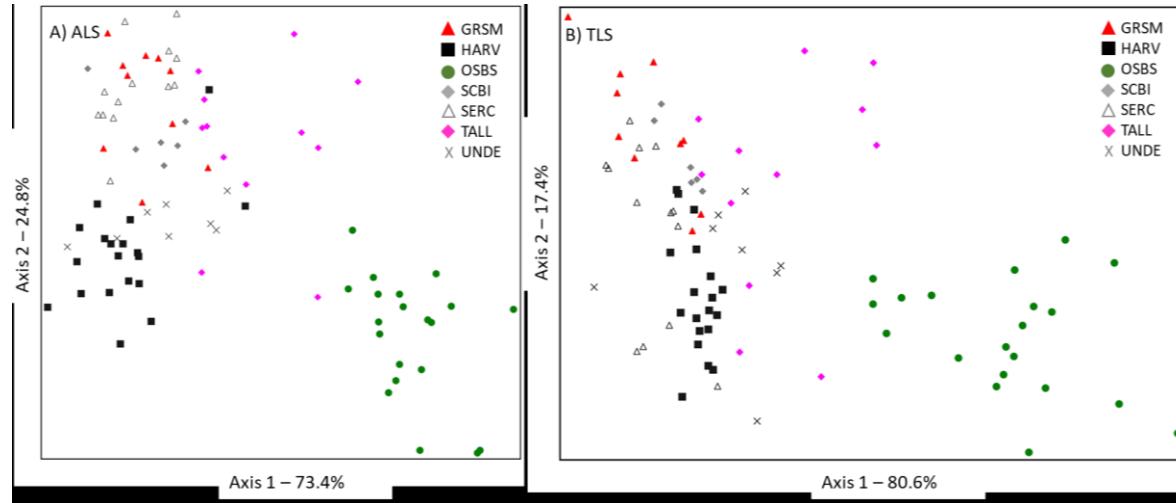
217 **Fig. 3.** Pairwise Spearman correlation coefficients between aerial laser scanning (ALS) (Y-axis) and
 218 terrestrial lasering scanning (TLS) metrics (X-axis). Boxes show the paired correlation coefficient
 219 results and the colors of the squares indicate the strength of each correlation; an X indicates a
 220 relationship was not significant at $\alpha < 0.05$.

221

222 3.2 Multivariate Comparison of ALS and TLS Classifications

223 There was strong agreement in the general multivariate classification of plots from different
 224 forest sites by ALS and TLS metrics of structural diversity (Fig. 4), demonstrating the ability of both
 225 systems to resolve forest type differences at the macroscale. NMS ordination of structural diversity
 226 derived from ALS data had a two-dimensional solution with a mean Stress of 7.811, which was
 227 significant relative to randomized data ($p = 0.004$) and explained a 98.2% of the variation in the
 228 original data matrix (Fig. 4A). The first axis explained 73.4% of the variation and was driven most
 229 strongly by VAI and maximum canopy height. The second axis explained an additional 24.8% of the
 230 variation and was most strongly driven by vertical variation in canopy height. There was relatively
 231 strong separation between sites in the ALS-based ordination space (Fig. 4A) and MRPP analysis
 232 indicated significant differentiation among sites in structural diversity ($A = 0.50$, $p < 0.001$).
 233 Classification of the TLS structural diversity metrics was also explained in two dimensions of
 234 multivariate structural space (Fig. 4B). The NMS ordination based on TLS structural diversity metrics
 235 had a two-dimensional solution that was significant relative to randomized data ($p = 0.004$; mean
 236 Stress = 8.665) and explained a 97.9 % of the variation in the original data matrix. The first axis
 237 explained 80.6% of the variation and was driven by vegetation area and openness. The second axis
 238 explained an additional 17.4% of the variation and was driven by canopy height and internal
 239 heterogeneity. NMS ordination of structural diversity derived from TLS data illustrated

240 differentiation among sites (MRPP analysis $A = 0.45$, $p < 0.001$). Both ALS and TLS suites of structural
 241 diversity metrics provided similar two-dimensional characterization of plots from different sites (c.f.
 242 Fig. 4A, 4B), indicating that both LiDAR systems are able to resolve differences in structural diversity
 243 of plots from different forest types at a sub-continental scale.



244
 245 **Fig. 4.** Non-metric multi-dimensional scaling ordination illustrating variation in multivariate
 246 classification of plots across seven studied forest sites from structural diversity as measured using a)
 247 aerial laser scanning (ALS) and b) terrestrial laser scanning (TLS). Site ID abbreviations can be found
 248 in Table 1.

249 While there was broad agreement in the clustering of plots from structurally similar forest
 250 sites that vary by height and openness from ALS and TLS metrics of structural diversity, the finer
 251 resolution of TLS data provided a greater ability to distinguish plots from within sites that have subtle
 252 differences in structural diversity (Fig. 5, Table 5). Hierarchical agglomerative clustering of TLS and
 253 ALS structural metrics produced different numbers of clusters in structural diversity space indicating
 254 that, as expected, TLS and ALS are sensitive to different canopy structural features. ALS structural
 255 diversity metrics were clustered into 3 groups (based on iterative indicator species analysis
 256 conducted on grouping levels; minimum average p-value in 3 cluster solution: $p = 0.0002$) (Table 5).
 257 These three groups separate plots from sites approximately by geography (latitude) with groups of
 258 northern (medium height and high canopy cover), mid-Atlantic/Appalachian (tallest height and high
 259 canopy cover), and southern sites (lowest height and open canopy) (Fig. 5A). In contrast, TLS
 260 structural diversity metrics grouped canopies into 5 clusters (minimum mean p-value from ISA – $p =$
 261 0.001) (Table 5). These clusters split the plots from the following groups of sites: HARV/SERC,
 262 GRSM/SERC, UNDE/SCBI, OSBS, and a subset of TALL (Fig. 5B). The additional groupings
 263 distinguished by the TLS data were related to plots with very tall canopy, but low complexity (cluster
 264 5 – TALL site), plots with short canopy, but high VAI (cluster 3 – largely at HARV and UNDE), and
 265 plots with extreme vertical complexity (cluster 2 – largely GRSM and SERC). Comparison of the
 266 groupings of plots into clusters using the two different data sets illustrated both substantial
 267 agreement in some regards and separation in others (Table 5). The two classification systems agreed
 268 in placing the OSBS plots into a distinct cluster group, while the other two ALS clusters aggregated
 269 plots largely from 2 or 3 of the TLS clusters respectively. The ability of the TLS to split plots from
 270 different sites into clusters with plots from other sites illustrates that TLS permits the characterization
 271

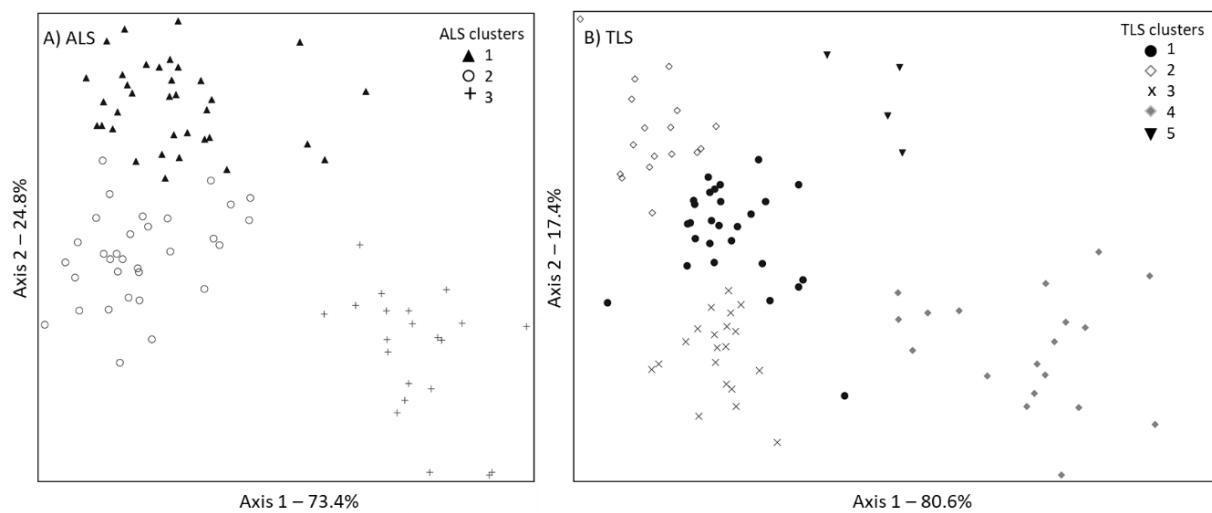
272 of within-site variability of structural diversity, versus the purely among-site variation that was
 273 represented in the ALS ordination and clustering (c.f. Fig. 5A, B).

274

275 **Table 5.** Comparison of plot assignment to groupings derived from hierarchical agglomerative
 276 clustering of aerial laser scanning (ALS) and terrestrial laser scanning (TLS) illustrating structural
 277 diversity variation in multivariate space between LiDAR platforms. Cluster name indicates which
 278 plot was assigned to a given TLS or ALS cluster. Numbers indicate the how many plots were assigned
 279 to each cluster.

Cluster	TLS1	TLS2	TLS3	TLS4	TLS5	Total
ALS1	12	15	4	0	4	35
ALS2	14	2	16	0	0	32
ALS3	1	0	0	20	0	21
Total	27	17	20	20	4	88

280



281

282 **Fig. 5.** Illustration of canopy structural type groupings derived from hierarchical agglomerative
 283 clustering overlaid on non-metric multi-dimensional scaling ordination of structural diversity across
 284 seven studied forest sites; A) illustrates cluster groups derived from aerial laser scanning (ALS) data
 285 and b) cluster groups from terrestrial laser scanning (TLS) data.

286 4. Discussion

287 Despite terrestrial and aerial LiDAR systems having trade-offs in their resolution and spatial
 288 extent for the characterization of structural diversity, the results of our study show broad agreement
 289 between ALS and TLS in the potential to quantify canopy structural diversity across a variety of forest

types at a sub-continental scale. We showed robust concurrence among equivalent measures of canopy height, cover and openness, vegetation area, and internal heterogeneity. We also show that ALS delineates the multivariate canopy structural types among forest sites at a sub-continental scale. Our results demonstrate that low resolution, large footprint ALS systems may be a useful tool for classifying forests by structural diversity at landscape to sub-continental scales. However, TLS derived metrics may be required to resolve fine-scale structural variation within forest types, such as that related to disturbance history, management, or successional development [34,45]. Previous studies have focused on comparisons of ALS and TLS at a single site or forest type in a localized region, but consistent with our results, these have found that ALS and TLS are comparable in their capacity to delineate features such as canopy height, cover, and vertical stratification [23,34–36]. TLS systems are a well-established method to provide high resolution, functionally meaningful measurements of structural diversity in forest ecosystems at the stand-scale [2,19,20,22,35,46], but these results demonstrate that ALS could potentially be used to scale the characterization of canopy structural diversity to much broader spatial extents.

The effects of occlusion that plague both bottom-up TLS and top-down ALS methods did not prevent robust agreement for 8 of the 10 equivalent metrics tested here, but did result in low agreement for two metrics of external heterogeneity. The top-down view of ALS versus the bottom-up viewing angle of TLS results in a difference of laser beam attenuation that may mean these systems see non-overlapping portions of the canopy volume (Fig. 1). Specifically, ALS typically exhibits decreased capacity to resolve subcanopy vegetation relative to TLS due to increased attenuation. However, ALS has been shown to be able to resolve layer differences in multi-level forest canopies in combination with robust predictive models [47]. Meanwhile, TLS exhibited a decreased ability to clearly characterize upper canopy elements relative to ALS also due increased attenuation [36]. The partial occlusion of the canopy surface in TLS data was apparent in our study, as univariate analyses illustrated only partial agreement among measures of external canopy heterogeneity that estimate structural diversity at the outer canopy surface. A similar issue was observed by Hilker et al. [23], who found that while TLS accurately measured canopy height from the top 10% of points, it underestimated total canopy height by approximately a meter. This suggests a need for caution in relying on the Portable Canopy TLS [22] for measuring outer canopy features (e.g. external heterogeneity), whereas ALS seems better suited for this category of structural diversity metric. Nevertheless, the broad agreement we observed between ALS and TLS methods for quantifying most categories of structural diversity metrics supports the use of ALS to scale up functionally relevant measurements of canopy structure, and further suggests that structural metrics derived from ALS can serve as a reasonable proxy for TLS derived metrics (e.g. [47]). Recent advances in new LiDAR technologies (e.g. full waveform LiDAR, Geiger mode, or USGS level-1 aggregates of a nominal pulse density 8 pts/m) and new computational algorithms are beginning to help reduce occlusion issues that hinder ALS, which may result in an even stronger agreement between ALS and TLS for measuring structural diversity. ALS is useful for measuring structural diversity metrics, however future research that incorporates these technological and computational advances could further improve the measurement of forest structural diversity.

The relatively low resolution of ALS is sufficient to distinguish between different forest sites based on multivariate structural diversity, but TLS is better suited to resolving within site variation. In our study there was a similar placement of plots from different forest types in multivariate space

333 based on ALS and TLS structural diversity metrics. These seven forest sites spanned an ecological
334 gradient across six of NEON's ecoclimatic domains, which may enhance our ability to identify unique
335 clusters of structural diversity types. However, there were both similarities and differences in the
336 hierarchical agglomerative clustering by TLS (5 clusters) and ALS (3 clusters). For example, OSBS, a
337 pine savannah characterized by open canopies and short trees, was always placed in its own cluster
338 by both LiDAR platforms. This illustrates the ability to clearly delineate general structural types
339 among different forests for ALS or TLS. Forest sites with denser canopies, dominated by deciduous
340 species (which tend to have broader, rounded crowns), did not cluster similarly and were split among
341 four TLS clusters and two from ALS. This indicates that studies seeking to investigate fine-scale
342 differences in structural diversity within a forest type or single site should rely on TLS to accurately
343 characterize sub-canopy structure. There are ecological and management circumstances for which it
344 is desirable to resolve fine-scale structural variation and its role in forest ecosystem function; for
345 example, to understand differences in local disturbance on the same forest type [34] or to assess the
346 effects of forest management actions [48]. However, previous studies have demonstrated that at
347 larger scales greater variation in structural diversity occurs across forest types and sites rather than
348 within sites [2,18,49]. For example, canopy structural types defined using multi-dimensional metrics
349 of three-dimensional forest structure are useful for predicting forest productivity [7]. The
350 applicability of ALS to delineate structural diversity types in forest transitional zones has yet to be
351 rigorously tested, but we hypothesize the within-type structural variability might be high while the
352 among-type variability would be low for different forest types. Transitional forest types on a
353 landscape-level would likely create additional clusters to those that we found in the ALS multivariate
354 analysis here. We suggest that the derivation of some canopy traits and general canopy structural
355 types across landscapes is feasible with ALS and that ALS could be an appropriate choice for
356 characterizing broad-scale forest variation in forest macrosystem studies (e.g. [50]). We also caution
357 users of ALS to keep the context of structural attributes of forests in mind, because resolving
358 structural diversity in the sub-canopy of open canopies will be easier than dense, closed canopies that
359 pose occlusion issues for low density ALS.

360 5. Conclusions

361 The TLS and ALS systems compared here each provide unique benefits for remotely sensing
362 forest structural diversity, and both can be robustly applied across different forest types at a sub-
363 continental scale. The portable canopy LiDAR TLS system we examined is extremely portable and
364 efficient at collecting within-canopy structural diversity data at stand scales—which makes this TLS
365 system useful in small-scale structural diversity analyses where higher point densities are needed.
366 The ALS system has the capacity to measure structural diversity at broader scales, which is
367 advantageous for investigating spatial and temporal dynamics or testing compatibility to model
368 simulations that use spaceborne remote sensing data at larger extents than is feasible to measure with
369 TLS systems. Furthermore, future studies should also compare remotely sensed measures of
370 structural diversity with forest-inventory based-structural diversity metrics (e.g. [9]), because forest
371 managers often make management decisions based predominantly on inventory metrics. Advances
372 in the open source coding and the accessibility of ALS, from organizations such as NEON, has a
373 distinct capacity to quantify forest canopy structural diversity at scales that have not been possible
374 until recently. These improvements allow for the incorporation of more comprehensive structural

375 information in ecological models, forest management, and strategic decision making for forest
376 macrosystems. Understanding the limitations and shortcomings of ALS and TLS LiDAR systems, and
377 how we can utilize the complementary strengths of these systems, is a critical step forward for further
378 understanding the complex dynamics that link forest structural diversity with macroscale patterns
379 of ecosystem functioning.

380 **Supplementary Materials:** The following are available online at www.mdpi.com/xxx/s1, Table S1. Derivation of
381 structural diversity metrics from aerial laser scanning (ALS). Supplementary methods: 1. Spatial stability of ALS
382 metrics estimated from the TLS 2D canopy slice approach, Figure S1: Breakpoint analysis for VAI, mean outer
383 canopy height, and maximum canopy height, Figure S2: Breakpoint analysis for top rugosity, standard deviation
384 of standard deviation of height, entropy, VCI, standard deviation of height, and rumple, Figure S3: Breakpoint
385 analysis for cover fraction, deep gaps, deep gap fraction, and gap fraction profile.

386 **Acknowledgements:** We thank three anonymous reviewers for improving the manuscript.

387 **Author Contributions:** SF and BH conceived the idea. FW and EL wrote the initial draft. EL, FW, JA, BF
388 conducted analyses. All authors contributed to writing and have approved the final version.

389 **Funding:** Funding for this work was supported by NSF award #1638702 to S. Fei and B. Hardiman, NSF award
390 #1924942 to S. Fei, B. Hardiman, and E. LaRue, NSF award # 1926538 to B. Hardiman, and USDA Forest Service
391 award #19-JV-11242305-102 to S. Fei.

392 **Conflicts of Interest:** The authors declare no conflict of interest.

393

394 **References**

395 1. LaRue, E.A.; Hardiman, B.S.; Elliott, J.M.; Fei, S. Structural diversity as a predictor of ecosystem function.
396 *Environ. Res. Lett.* **2019**, *14*.

397 2. Atkins, J.W.; Bohrer, G.; Fahey, R.T.; Hardiman, B.S.; Morin, T.H.; Stovall, A.E.L.; Gough, C.M.
398 Quantifying vegetation and canopy structural complexity from TLS data using the forestr r package.
399 *Methods Ecol. Evol.* **2018**, *9*, 2057–2066.

400 3. Niinemets, U. Photosynthesis and resource distribution through plant canopies. *PLANT CELL Environ.*
401 **2007**, *30*, 1052–1071.

402 4. Matheny, A.M.; Bohrer, G.; Garrity, S.R.; Morin, T.H.; Howard, C.J.; Vogel, C.S. Observations of stem
403 water storage in trees of opposing hydraulic strategies. *Ecosphere* **2015**, *6*, art165.

404 5. Hardiman, B.S.; Gough, C.M.; Halperin, A.; Hofmeister, K.L.; Nave, L.E.; Bohrer, G.; Curtis, P.S.
405 Maintaining high rates of carbon storage in old forests: A mechanism linking canopy structure to forest
406 function. *For. Ecol. Manage.* **2013**, *298*, 111–119.

407 6. Fotis, A.T.; Morin, T.H.; Fahey, R.T.; Hardiman, B.S.; Bohrer, G.; Curtis, P.S. Forest structure in space
408 and time: Biotic and abiotic determinants of canopy complexity and their effects on net primary
409 productivity. *Agric. For. Meteorol.* **2018**, *250*, 181–191.

410 7. Fahey, R.T.; Atkins, J.W.; Gough, C.M.; Hardiman, B.S.; Nave, L.E.; Tallant, J.M.; Nadehoffer, K.J.; Vogel,
411 C.; Scheuermann, C.M.; Stuart-Haëntjens, E.; et al. Defining a spectrum of integrative trait-based
412 vegetation canopy structural types. *Ecol. Lett.* **2019**, *22*, 2049–2059.

413 8. Ehbrecht, M.; Schall, P.; Ammer, C.; Seidel, D. Quantifying stand structural complexity and its
414 relationship with forest management, tree species diversity and microclimate. *Agric. For. Meteorol.* **2017**,
415 *242*, 1–9.

416 9. McElhinny, C.; Gibbons, P.; Brack, C.; Bauhus, J. Forest and woodland stand structural complexity: Its
417 definition and measurement. *For. Ecol. Manage.* **2005**, *218*, 1–24.

418 10. Atkins, J.W.; Bohrer, G.; Fahey, R.T.; Hardiman, B.S.; Gough, C.M.; Morin, T.H.; Stovall, A.; Zimmerman,
419 N. Forestr: ecosystem and canopy structural complexity metrics from LiDAR. *R Packag. version* **2018**, *1*.

420 11. Wilkes, P.; Disney, M.; Vicari, M.B.; others Estimating urban above ground biomass with multi-scale
421 LiDAR. *Carbon Balanc. Manag.* **2018**, *13*, 10.

422 12. Fisher, R.A.; Koven, C.D.; Anderegg, W.R.L.; Christoffersen, B.O.; Dietze, M.C.; Farrior, C.E.; Moorcroft,
423 P.R. Vegetation demographics in Earth System Models: A review of progress and priorities. *Glob. Chang.
424 Biol.* **2018**, *24*, 35–54.

425 13. Shiklomanov, A.N.; Bradley, B.A.; Dahlin, K.M.; M Fox, A.; Gough, C.M.; Hoffman, F.M.; M Middleton,
426 E.; Serbin, S.P.; Smallman, L.; Smith, W.K. Enhancing global change experiments through integration of
427 remote-sensing techniques. *Front. Ecol. Environ.* **2019**, *17*, 215–224.

428 14. Lefsky, M.A.; Cohen, W.B.; Harding, D.J.; Parker, G.G.; Acker, S.A.; Gower, S.T. LiDAR remote sensing
429 of above-ground biomass in three biomes. *Glob. Ecol. Biogeogr.* **2002**, *11*, 393–399.

430 15. Lim, K.; Treitz, P.; Wulder, M.; St-Onge, B.; Flood, M. LiDAR remote sensing of forest structure. *Prog.*
431 *Phys. Geogr. Earth Environ.* **2003**, *1*, 88–106.

432 16. Nguyen, H.T.; Hutyra, L.R.; Hardiman, B.S.; Raciti, S.M. Characterizing forest structure variations across
433 an intact tropical peat dome using field samplings and airborne LiDAR. *Ecol. Appl.* **2016**, *26*, 587–601.

434 17. Disney, M.I.; Boni Vicari, M.; Burt, A.; Calders, K.; Lewis, L.; Raumonen, P.; Wilkes, P. Weighing trees
435 with lasers: advances, challenges and opportunities. *Interface Focus* **2018**, *8*, 20170048.

436 18. LaRue, E.A.; Atkins, J.W.; Dahlin, K.; Fahey, R.; Fei, S.; Gough, C.; Hardirnan, B.S. Linking Landsat to
437 terrestrial LiDAR: Vegetation metrics of forest greenness are correlated with canopy structural
438 complexity. *Int. J. Appl. EARTH Obs. Geoinf.* **2018**, *73*, 420–427.

439 19. Paynter, I.; Genest, D.; Saenz, E.; Peri, F.; Boucher, P.; Li, Z.; Strahler, A.; Schaaf, C. Classifying
440 ecosystems with metaproperties from terrestrial laser scanner data. *Methods Ecol. Evol.* **2018**, *9*, 210–222.

441 20. Newnham, G.J.; Armston, J.D.; Calders, K.; Disney, M.I.; Lovell, J.L.; Schaaf, C.B.; Strahler, A.H.; Danson,
442 F.M. *Terrestrial Laser Scanning for Plot-Scale Forest Measurement*; Springer: New York, 2015; ISBN 3.

443 21. Lefsky, M.A.; Cohen, W.B.; Parker, G.G.; Harding, D.J. LiDAR remote sensing for ecosystem studies.
444 *Bioscience* **2002**, *52*, 19–30.

445 22. Parker, G.G.; Harding, D.J.; Berger, M.L. A portable LiDAR system for rapid determination of forest
446 canopy structure. *J. Appl. Ecol.* **2004**, *41*, 755–767.

447 23. Hilker, T.; Coops, N.C.; Newnham, G.J.; van Leeuwen, M.; Wulder, M.A.; Stewart, J.; Culvenor, D.S.
448 Comparison of terrestrial and airborne LiDAR in describing stand structure of a thinned lodgepole pine
449 forest. *J. For.* **2012**, *110*, 97–104.

450 24. Wing, B.M.; Ritchie, M.W.; Boston, K.; Cohen, W.B.; Gitelman, A.; Olsen, M.J. Prediction of understory
451 vegetation cover with airborne lidar in an interior ponderosa pine forest. *Remote Sens. Environ.* **2012**, *124*,
452 730–741.

453 25. Ferraz, A.; Bretar, F.; Jacquemoud, S.; Gonçalves, G.; Pereira, L.; Tomé, M.; Soares, P. 3-D mapping of a
454 multi-layered Mediterranean forest using ALS data. *Remote Sens. Environ.* **2012**, *121*, 210–223.

455 26. Campbell, M.J.; Dennison, P.E.; Hudak, A.T.; Parham, L.M.; Butler, B.W. Quantifying understory
456 vegetation density using small-footprint airborne lidar. *Remote Sens. Environ.* **2018**, *215*, 330–342.

457 27. Venier, L.A.; Swystun, T.; Mazerolle, M.J.; Kreutzweiser, D.P.; Wainio-Keizer, K.L.; McIlwrick, K.A.;
458 Woods, M.E.; Wang, X. Modelling vegetation understory cover using LiDAR metrics. *PLoS One* **2019**, *14*,
459 1–17.

460 28. Hamraz, H.; Contreras, M.A.; Zhang, J. Forest understory trees can be segmented accurately within

461 sufficiently dense airborne laser scanning point clouds. *Sci. Rep.* **2017**, *7*, 1–9.

462 29. Hamraz, H.; Contreras, M.A.; Zhang, J. Vertical stratification of forest canopy for segmentation of
463 understory trees within small-footprint airborne LiDAR point clouds. *ISPRS J. Photogramm. Remote Sens.*
464 **2017**, *130*, 385–392.

465 30. Kankare, V.; Vauhkonen, J.; Tanhuanpää, T.; Holopainen, M.; Vastaranta, M.; Joensuu, M.; Krooks, A.;
466 Hyppä, J.; Hyppä, H.; Alho, P.; et al. Accuracy in estimation of timber assortments and stem
467 distribution - A comparison of airborne and terrestrial laser scanning techniques. *ISPRS J. Photogramm.*
468 *Remote Sens.* **2014**, *97*, 89–97.

469 31. Trochta, J.; Kruček, M.; Vrška, T.; Kraál, K. 3D Forest: An application for descriptions of three-
470 dimensional forest structures using terrestrial LiDAR. *PLoS One* **2017**, *12*, 1–17.

471 32. Wang, Y.; Lehtomäki, M.; Liang, X.; Pyörälä, J.; Kukko, A.; Jaakkola, A.; Liu, J.; Feng, Z.; Chen, R.;
472 Hyppä, J. Is field-measured tree height as reliable as believed – A comparison study of tree height
473 estimates from field measurement, airborne laser scanning and terrestrial laser scanning in a boreal
474 forest. *ISPRS J. Photogramm. Remote Sens.* **2019**, *147*, 132–145.

475 33. Liang, X.; Wang, Y.; Pyörälä, J.; Lehtomäki, M.; Yu, X.; Kaartinen, H.; Kukko, A.; Honkavaara, E.; Issaoui,
476 A.E.I.; Nevalainen, O.; et al. Forest in situ observations using unmanned aerial vehicle as an alternative
477 of terrestrial measurements. *For. Ecosyst.* **2019**, *6*, 20.

478 34. Listopad, C.M.C.S.; Drake, J.B.; Masters, R.E.; Weishampel, J.F. Portable and airborne small footprint
479 LiDAR: Forest canopy structure estimation of fire managed plots. *Remote Sens.* **2011**, *3*, 1284–1307.

480 35. Hopkinson, C.; Lovell, J.; Chasmer, L.; Jupp, D.; Kljun, N.; van Gorsel, E. Integrating terrestrial and
481 airborne LiDAR to calibrate a 3D canopy model of effective leaf area index. *Remote Sens. Environ.* **2013**,
482 *136*, 301–314.

483 36. Hilker, T.; van Leeuwen, M.; Coops, N.C.; Wulder, M.A.; Newnham, G.J.; Jupp, D.L.B.; Culvenor, D.S.
484 Comparing canopy metrics derived from terrestrial and airborne laser scanning in a Douglas-fir
485 dominated forest stand. *Trees - Struct. Funct.* **2010**, *24*, 819–832.

486 37. Braun, L. *Deciduous Forests of Eastern North America*; Hafner: New York, 1950;

487 38. Atkins, J.W.; Fahey, R.T.; Hardiman, B.S.; Gough, C.M. Forest Canopy Structural Complexity and Light
488 Absorption Relationships at the Subcontinental Scale. *J. Geophys. Res. Biogeosciences* **2018**, *123*, 1387–1405.

489 39. Team, R.D.C. R: A language and environment for statistical computing. R Foundation for Statistical
490 Computing, Vienna, Austria, ISBN 3-900051-07-0. <http://www.R-project.org>. **2019**.

491 40. Network., N.E.O. Data Products: DP1.30003.001. Provisional data downloaded from
492 <http://data.neonscience.org> on January 1, 2019. Battelle, Boulder, CO, USA. **2019**.

493 41. Roussel, J.R.; Auty, D. LidR: Airborne LiDAR data manipulation and visualization for forestry
494 applications. *R Packag. version* **2018**, *1*, 1.

495 42. Silva, C.A.; Crookston, N.L.; Hudak, A.T.; Vierling, L.A.; Klauberg, C.; Cardil, A. rLiDAR: LiDAR data
496 processing and visualization. *R Packag. version 0*. **2017**, 1, 1.

497 43. McCune, B.; Mefford, M.J. PC-ORD. Multivariate analysis of Ecological Data, Version 5.0 for Windows.
498 MjM Software, Gleneden Beach, Oregon, U.S.A. **2006**.

499 44. McCune, B.; Grace, J. Analysis of ecological communities. MJM Software Design, Gleneden Beach, OR
500 2002.

501 45. Meadows, M.E.; Hill, T.R. Issues in Biogeography: Diversity in theory and practice. *South African Geogr.*
502 *J.* **2012**, 6245, 116–124.

503 46. Paynter, I.; Saenz, E.; Genest, D.; Peri, F.; Erb, A.; Li, Z.; Wiggin, K.; Muir, J.; Raumonen, P.; Schaaf, E.S.;
504 et al. Observing ecosystems with lightweight, rapid-scanning terrestrial lidar scanners. *Remote Sens. Ecol.*
505 *Conserv.* **2016**, 2, 174–189.

506 47. Mund, J.-P.; Wilke, R.; Körner, M.; Schultz, A. Detecting Multi-layered Forest Stands Using High Density
507 Airborne LiDAR Data. *GI_Forum* **2015**, 1, 178–188.

508 48. Donager, J.J.; Sankey, T.T.; Sankey, J.B.; Meador, S.; E., A.; Springer, A.J.; Bailey, J.D. Examining forest
509 structure with terrestrial lidar: Suggestions and novel techniques based on comparisons between
510 scanners and forest treatments. *Earth Sp. Sci.* **2018**, 10, 753–776.

511 49. Gough, C.M.; Atkins, J.W.; Fahey, R.T.; Hardiman, B.S. High rates of primary production in structurally
512 complex forests. *Ecology* **2019**, 100, e02864.

513 50. Kleindl, W.; Stoy, P.; Binford, M.W.; Desai, A.R.; Dietze, M.C.; Schultz, C.A.; Starr, G.; Staudhammer,
514 C.L.; Wood David J. A. Toward a Social-Ecological Theory of Forest Macrosystems for Improved
515 Ecosystem Management. *For. v.* **2018**, 9.

516



© 2020 by the authors. Submitted for possible open access publication under the terms and conditions of the Creative Commons Attribution (CC BY) license (<http://creativecommons.org/licenses/by/4.0/>).